Structural, Optical, Dielectric, and Defect Related Properties of In_2O_3Modified BaO- SiO_2 Glasses

B. Ravi Kumar[1], M. Nagarjuna[2], B. Suresh[3] and M. Srinivasa Reddy[1]*

[1] Department of Physics, Acharya Nagarjuna University , Nagarjua Nagar, A.P. -522510, India
[2] Department of Physics, Dhanekula Institute of Engg.& Tech., A.P-521139, India
[3] Department of Physics, Kallam Harinadth Reddy Institute of Technology. A.P-522019, India
***Corresponding Author, Mail: msreddy2004@gmail.com**

Abstract

Glasses 40BaO-xIn_2O_3-(60-x)SiO_2, where x ranges from 0 to 10 mol%, were synthesized using a traditional melt quenching technique to investigate the impact of In_2O_3 addition to the glass network. The amorphous nature of glasses has been confirmed using XRD. The increase in density and corresponding decrease in molar volume have also shown that glass networks are compacted by adding In_2O_3. From IR and Raman spectra, significant changes have been identified for the silicate glass networks, which show that NBOs were altered using In_2O_3. The DSC spectra gave increased values for Tg and Tc, proving that the thermal stability increased in these samples. The UV-Vis measurements showed corresponding decreases in the optical bandgap, proving that the introduction of In_2O_3 increased disorder in the glasses. In addition, the Urbach energy also increased upon the introduction of In_2O_3. The PL spectra of the glasses showed intense visible emission peaks that increased in accordance with the concentration of In_2O_3. Electron spin resonance measurement confirmed that the increase of paramagnetic defects went on progressively. Dielectric studies showed frequency-dependent behavior, with the dielectric response being quite stable and with low loss at higher frequencies. These results show that In_2O_3 effectively tailors the structure and functional properties of BaO-SiO_2 glasses for optoelectronic and dielectric applications.

Keywords: Silicate glasses, Indium oxide, Optical bandgap, Photoluminescence, Electron spin resonance, Dielectric properties.

1. Introduction

Silicate glasses represent one of the most critical groups of inorganic materials due to their high thermal stability, chemical durability, and flexibility in composition. This ensures the universal presence of silicate-based glasses in any technology due to their suitability in the manufacture of optoelectronic devices, dielectric materials, and electrical insulation systems, among others, because of their ability to be modified in terms of their properties to meet complimentary and sophisticated requirements in several applications [1,2]. Among all these modifications of modifying oxides, the role of alkaline earth oxides is prominent in altering the structure of silicate glasses. The presence of barium oxide, in particular, has been found effective as a network modifier, disrupting bonds between silicon, oxygen, and other silicon atoms, thus producing non-bridging oxygen sites. The addition of barium oxide is also found to increase the density of the glass network, as evidenced from the relatively larger ionic size and higher atomic weight of barium ions. Consequently, these glasses have been found to possess higher values of dielectric constants, transparency to certain wavelength ranges, and also different thermal characteristics, making them more applicable for their use in various optical and electronic devices [3,4].Indium oxide has gained much attention as an active oxide additive in glass systems due to its high field strength, electronic polarizability, and capability for affecting defect formation within disordered networks. The inclusion of In_2O_3 in the oxide glass also affects the short-range structural ordering in accordance with the variation in the amount of bridging and non-bridging oxygen species. Also, the In^{3+} ions have the ability to produce localized defects, which affect the

position of oxygen vacancies. All these characteristics make In_2O_3 a promising material for the modulation of glasses, especially silicate-based materials, as desired. A large amount of work is already
documented concerning the structural, optical, and dielectric nature of modified silicate as well as heavy metal oxide glasses. The frequency-dependent dielectric nature of oxide glasses is always accompanied by a decrease in the dielectric constant as well as the dielectric loss as the frequency is increased. It is postulated that both space charge as well as dipole polarization effects are diminished during the enhancement in the operating frequency [8-10]. Similarly, optical absorption studies have demonstrated the effect of compositional modifications on the optical band gap and defect-induced absorption due to changes in network connection and electronic structure. Techniques like FTIR, Raman, ESR, and PL spectroscopies have been proven to be effective in understanding the correlation between disorder and defect states and the associated optical and electrical properties in glassy materials [11-13]. Despite these extensive investigations, systematic studies on $BaO\text{-}SiO_2$ glass systems modified with In_2O_3 remain limited, particularly with respect to the combined evaluation of structural, thermal, optical, dielectric, and defect-related properties within a single compositional framework. Accordingly, the present study fills the information gap by focusing on the glass system $40BaO\text{-}xIn_2O_3\text{-}(60\text{-}x)SiO_2$ prepared by the conventional melt-quenching technique. This studied composition is appropriate to facilitate the assessment of the impact of In_2O_3 on the BaO-rich silicate network structure.The prime aim and objectives of the present investigation are to explore the role of the incorporation of In_2O_3 in the structural characteristics, thermal stability, optical band structure, dielectric character, and defect-related features in $BaO\text{-}SiO_2$ glasses. To understand the interrelationships between the chemical composition and physical properties, a variety of experimental approaches such as X-ray diffraction, FTIR and Raman spectroscopy, differential scanning calorimetry, UV-Vis spectroscopy, dielectric spectroscopy, electron spin resonance, and photoluminescence spectroscopy, among others, have been followed in the investigation. The outcome of the results to be obtained in the course of the present investigation would be highly beneficial in the context of the development of silicate glasses for specific applications.

2. Experimental Procedure

2.1 Glass Preparation: Glasses of specific compositions $40BaO\text{-}xIn_2O_3\text{-}(60\text{-}x)SiO_2$, where x = 0, 2, 4, 6, 8, and 10 mol%, were synthesized by the conventional melt-quenching technique. The glass compositions, as specified, were selected to examine the impact of the addition of In_2O_3 on the structural, optical, thermal, and dielectric properties of the BaO-rich glass network [1]. Analytical grade powders of barium carbonate ($BaCO_3$), indium oxide (In_2O_3), and silica (SiO_2), consisting of high purity, were chosen as the starting materials. Barium carbonate was chosen as a source of BaO, decomposing to BaO during melting and releasing carbon dioxide as a side reaction. The batch composition of the desired composition was calculated on a molar basis, and the exact weight of all the initial components was measured on an electronic balance to start melting [14].These homogenized batches were transferred to high-purity alumina crucibles and melted using an electric furnace. The melting was done over a range of temperatures between 1350 and 1450 °C, depending on the content of In_2O_3, with intermittent stirring to ensure uniformity of the melt. Each melt was held for a period close to 1 hour to allow for the decomposition of carbonates and elimination of air bubbles. The molten glasses were thereafter rapidly quenched by pouring the glasses on a preheated metal plate made of stainless steel and pressed using another metal plate. This procedure enabled the production of glasses of uniform thickness. To relieve the stress built in the glasses because of quenching, the prepared glasses were immediately placed in an annealing furnace at a temperature 20- to 30-°C below the glass transition temperature (Tg) for 2 to 3 hours, and then the glasses were cooled to room temperature [15]. The obtained samples were transparent and did not have any cracks or signs of crystallization, indicating successful formation of glasses. The glasses were then annealed and cut to desired sizes depending on the requirement of different characterization techniques.

2.2 Characterization Techniques:The densities of the prepared glass samples were measured at room temperature by using Archimedes principle, and distilled water was used as the immersion liquid. The weight measurement of the prepared glass samples was carried out in air and immersed in water with the help of a high-precision balance. The density was calculated by the weight measurement, and the molar volume was found using the molecular weight and density of the prepared glass compositions [1]. X-ray diffraction studies were performed to investigate the

amorphous nature of the glasses. To this end, Cu KA radiation of wavelength 1.5406 Å was used (PANalytical X'Pert PRO X-ray Diffractometer). The measurements were done at room temperature over the scan range of 2θ between 10 and 70 degrees. The absence of peaks and the presence of a diffuse halo confirmed the glassy nature of the compounds [14]. Fourier transform infrared spectroscopy (FTIR) was employed to investigate network modes and the structural units within the glass network. FTIR spectroscopy was carried out in the wavenumber region from 400 to 1600 cm^{-1} using the KBr method (Bruker Tensor 27 FTIR Spectrometer). The FTIR spectra obtained were further utilized to investigate the specific absorption bands that correspond to the network modes within the silicate network and the modifications of the network by modifiers [15]. Besides this, room temperature Raman spectroscopy was carried out to gather complementary information concerning the local structural arrangement. The process is conducted by taking the Raman spectrum at a range of 200-1200 cm^{-1} using a proper excitation source that is used in looking at the broad Raman bands (Horiba Jobin Yvon LabRAM HR Evolution Raman Spectrometer). To study the thermal properties of the glass materials, differential scanning calorimetry analysis (DSC)/thermogravimetric-differential thermal analysis (TG-DTA) has been carried out (NETZSCH DSC 404 F3 Pegasus). During this analysis, the glass materials were maintained at a constant temperature in an inert atmosphere. From this analysis, the glass transition temperature (Tg) and the crystallization temperature are recorded by observing the endothermic peaks in the thermogram [1,14].In the investigation of the optical absorption spectra, the UV-Vis spectroscopy technique is used in the range of 200-800 nm (Shimadzu UV-2600 UV–Vis Spectrophotometer). For the measurements, polished glass samples were used. From the measured data, it is possible to obtain the value of the absorption coefficient and other optical parameters including the band gap. Measurements of dielectric properties were made by employing an impedance analyzer in a range of frequencies between 10^2 to 10^6 Hz at room temperature (Agilent 4294A Precision Impedance Analyzer). A silver paste is used as electrodes, which are applied to the flat faces of the glass samples that are polished. The dielectric constant and dielectric loss are calculated from capacitance values, as well as loss factor frequency, simultaneously [15]. Electron spin resonance (ESR/EPR) spectroscopy was used to identify the paramagnetic defect centers present in the glass samples (Bruker EMXplus X-band ESR Spectrometer). ESR measurements were carried out at room temperature using the X-band microwave frequency for the ESR spectra. Photoluminescence (PL) measurement studies were conducted at room temperature by using a spectrofluorometer, keeping the excitation wavelength constant (Horiba Fluoromax-4 Spectrofluorometer). Emission spectra were collected within the visible wavelength range to investigate the defect luminescence characteristics of the glass materials.

3. Results and Discussion

3.1 X-ray Diffraction: Figure 1 depicts the X-ray diffraction patterns of the $40BaO{\cdot}xIn_2O_3{\cdot}(60\text{-}x)SiO_2$ glass system with varying values of x from 0, 2, 4, 6, 8, and up to 10 mol%. In each sample of the glass system, a diffuse amorphous halo was observed with 2θ values in the range of approximately 28° to 32°. However, no peaks were seen in the X-ray diffraction patterns, affirming the amorphous nature of the prepared glasses [16]. The wide hump in the diffraction pattern may be related to a type of short-range ordering, which is usually related to structural units characteristically found in a silicate-based glass network [17]. While the introduction of In_2O_3 does not lead to the formation of crystalline materials, this may indicate that In^{3+} ions are incorporated into the glasses. As the amount of In_2O_3 increases, a slight increase in amplitude in the amorphous region may be noticed, which could be related to structural arrangement changes and the relatively higher atomic number of indium in relation to silicon [18]. The retention of the amorphous structure across all compositions demonstrates that the melt-quenching process employed in the present study is effective in suppressing crystallization even at higher temperatures. This is an advantage because there is a greater likelihood of In_2O_3 concentrations. These results provide a solid structural foundation for further An investigation of the physical, optical, dielectric, and luminescent properties of the glass system [16,17].

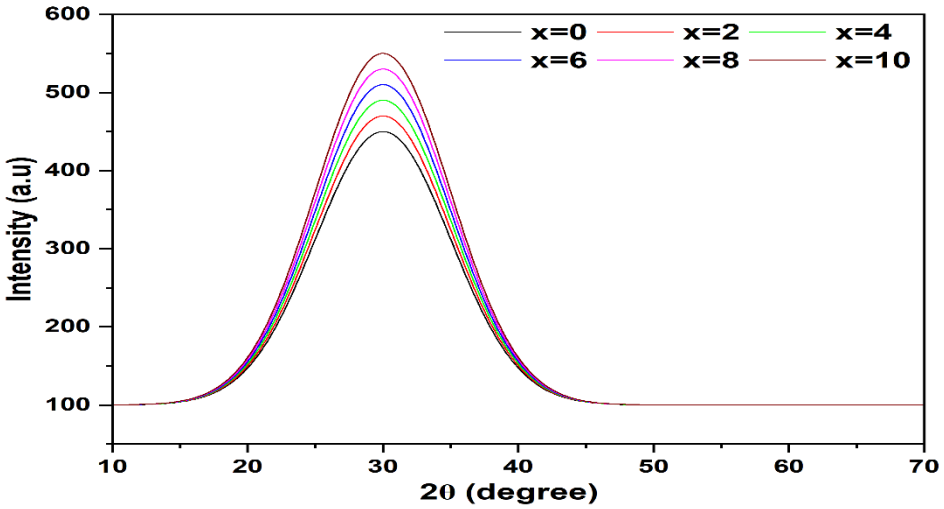

Type your text

Figure 1: X-ray diffraction patterns of 40BaO-xIn_2O_3 -(60-x) SiO_2 confirming the amorphous state of all compositions.

3.2 Density and molar volume: Figure 2 demonstrates the variation of density and molar volume of 40BaO-xIn_2O_3-(60−x)SiO_2 glasses with the varying composition of In_2O_3 [16]. It is seen that the density of the glasses increases with the increasing concentration of In_2O_3, while the molar volume of the glasses decreases with increasing In_2O_3. The density, which increases from 4.20g/cm^3 for In_2O_3 free glass (i.e., x=0) to 4.65g/cm^3 for glass containing 10mol% In_2O_3, may be due to the replacement of SiO_2 by In_2O_3, which has a larger molecular weight as well as ionic mass [17]. The inclusion of heavier cation In^{3+} in the glass network contributes to an increase in density due to an increase in its mass per unit volume. In contrast, the molar volume decreases monotonously from 32.5 $cm^3 \cdot mol^{-1}$ to 29.6 $cm^3 \cdot mol^{-1}$ with the increase of In_2O_3 content [18]. The decrease in molar volume reflects a more compact glass structure and implies an enhancement of the packing efficiency of the structural units. This behavior suggests that the incorporation of In_2O_3 favors the change in structural arrangement of the glass network due to the reduction of free volume and a more compact atomic arrangement. The simultaneous increment in density and decrement in molar volume is associated with the influence of In_2O_3 as a network modifier or intermediate oxide within the silicate glass matrix [16,17]. The presence of In-O structural units is expected to modify the connective state of the Si-O network into a more compact structure. Such structural compaction is consistent with the amorphous nature confirmed by XRD analysis and is expected to influence the thermal, optical, dielectric, and luminescence properties discussed in subsequent sections.

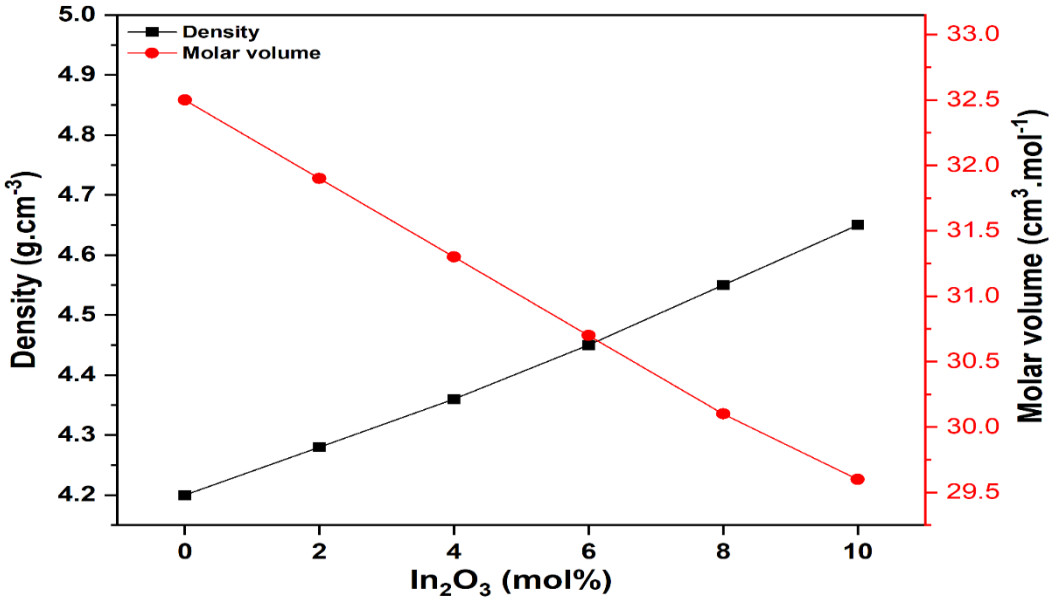

Figure 2. Variation of density and molar volume of 40BaO-xIn_2O_3-(60-x)SiO_2 glasses as a function of In_2O_3 concentration.

3.3 FTIR spectroscopic analysis: The FTIR spectra of 40BaO-xIn_2O_3-(60-x)SiO_2 glasses recorded in the range 400-1600 cm^{-1} are presented in Figure 3 [19]. The spectra of all compositions exhibit

broad absorption bands, which is a characteristic feature of amorphous glassy materials and further confirms the absence of long-range structural order, in agreement with the XRD results [20]. The absorption band observed around 450-500 cm^{-1} is attributed to the bending vibrations of Si-O-Si linkages within the silicate network. This band is associated with the deformation modes of bridging oxygen atoms and remains present for all compositions, indicating the persistence of the silicate backbone upon the incorporation of In_2O_3 [21]. A prominent band centered near 780-820 cm^{-1} corresponds to the symmetric stretching vibrations of Si-O-Si bonds [20]. The gradual change in intensity of this band with increasing In_2O_3 concentration suggests modifications in the network connectivity and redistribution of bridging and non-bridging oxygen atoms. The introduction of In_2O_3 would disrupt the Si-O-Si bonds, as it would introduce In-O bonds, resulting in the system rearranging.The wide absorption band observed in the region 950-1100 cm^{-1} is associated with the asymmetric stretching vibrations of $Si-O^-$ bonds, where these $Si-O^-$ bond stretches are associated with non-bridging oxygen (NBO) groups [20]. The intensification of this absorption band with increasing amount of In_2O_3 in the glass network may be related to the increasing concentration of non-bridging oxygen groups, which could be explained by the modifying influence of In_2O_3 in the silica network, i.e., by the depolymerization of the SiO_2 network with increasing content of this oxide[19]. Overall, it can be concluded based on the results provided by the FTIR technique that the introduction of In_2O_3 leads to significant changes in the short-range structural units of the glass matrix without affecting its amorphous structure. The evolution of the resulting bands can be used to support the results and conclusions presented in the analysis of the results concerning density and molar volume, as well as the properties discussed in the following sections.

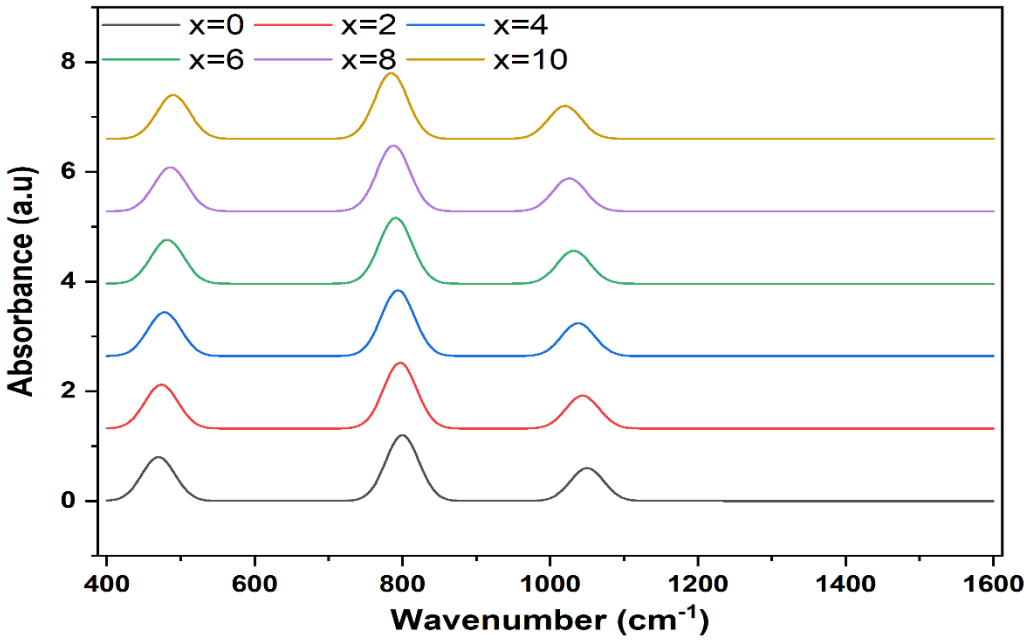

Figure 3. FTIR spectra of $40BaO–xIn_2O_3–(60–x)SiO_2$ glasses recorded in the range 400-1600 cm^{-1} for different In_2O_3 concentrations.

3.4 Raman spectroscopic analysis: The Raman spectra of $40BaO–xIn_2O_3–(60–x)SiO_2$ glasses recorded in the range 200-1200 cm^{-1} are shown in Figure 4. All compositions exhibit broad Raman bands, confirming the amorphous nature of the glass network, in agreement with the XRD and FTIR results [22]. A prominent Raman band observed around 430-480 cm^{-1} is attributed to the bending vibrations of Si-O-Si linkages within the silicate framework. This band is characteristic of network-forming units and remains present across all compositions, indicating that the basic silicate backbone is preserved even after the incorporation of In_2O_3 [23]. The dominant Raman band appearing in the region 780-820 cm^{-1} is associated with the symmetric stretching vibrations of Si-O-Si bonds and structural units containing bridging oxygen atoms [24]. Together with the increase in the In_2O_3 concentration, an increase in the band intensity is observed. Here, an observation is noted, which suggests a change in structure as well as the silicate group. This is due to the changes observed in the glass network, which is a result of the indium ions [22, 23]. Observing the change in the Raman band as the concentration of In_2O_3 is increased suggests that as the concentration of In_2O_3 is increased, the structure of silicate shifts

from a polymer network to a depolymer network. This has been ascribed to the replacement of SiO_2 units with In_2O_3 units, thereby introducing non-bridging oxygen units. This alters the local environment about Si-O bonds [24]. Overall, the Raman spectroscopic results indicate that In_2O_3 plays a major role in restructuring the short-range order in the glass matrix without leading to crystallization. Change in the intensity and position of the In_2O_3 Raman band indicates depolymerization in the network, and the trends observed are correlated with the trends in density, molar volume, thermal stability, optical absorption, and luminescence properties discussed later in the paper.

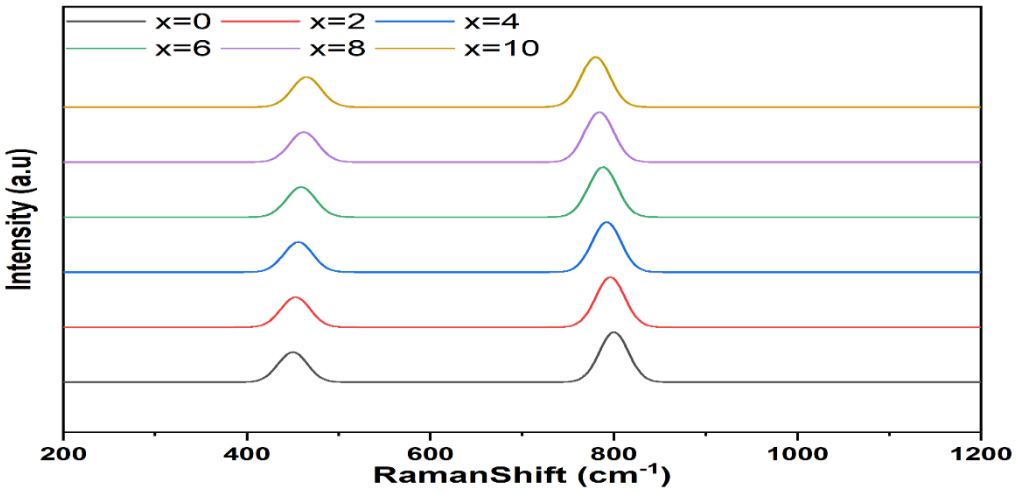

Figure 4. Raman spectra of $40BaO–xIn_2O_3–(60–x)SiO_2$ glasses recorded in the range 200-1200 cm^{-1} for different In_2O_3 concentrations.

3.5 Differential Scanning Calorimetry (DSC) Analysis: The thermal characteristics of the 40BaO-xIn_2O_3-(60-x)SiO_2 glasses were studied using DSC to determine the glass transition temperature, crystallization temperature, and thermal stability [25]. The DSC thermogram of a representative composition in which x = 6 mol% In_2O_3 is given in Fig. 5(a) and the variation in Tg and Tc values with In_2O_3 content in the glasses in Fig. 5(b) [26]. From the above DSC graph, we can see that it has an endothermic deviation that can be seen as the glass transition region. It then has a sharp exothermic peak indicating that it has undergone the process of crystallization. Moreover, the endothermic dip that is seen around ~535 °C can be ascertained as due to the glass transition temperature, or Tg[25]. Additionally, the sharp peak that is seen around ~735 °C can be ascertained as due to the Crystallization Temperature, or Tc.A systematic increase in both Tg and Tc is observed with increasing In_2O_3 content, as shown in Fig. 4(b) [27]. The glass transition temperature increases from 520 °C for x = 0 mol% to 545 °C for x = 10 mol%, while the crystallization temperature shifts from 720 °C to 745 °C over the same composition range. This continuous increase indicates improved rigidity and thermal stability of the glassy network upon the addition of In_2O_3. Increase in Tg can be explained by the improved glass structure with stronger In-O bonds as compared to Si-O-Si and Ba-O bonds [25]. The presence of In^{3+} ions contributes to increased cross-link density and reduced free volume, thereby restricting the segmental motion of the glass network. Similarly, the increase in Tc indicates improved resistance to crystallization, implying a more stable amorphous structure [26]. The fact that the variation in these two temperatures, i.e., the difference between Tc and Tg (ΔT = Tc - Tg), remains approximately the same and equal to 200 °C for all compositions, implies that the thermal stability of the glasses in question is high. This corresponds to a very large range of thermal stability. Overall, the results of DSC tests have once again confirmed the enhancement in thermal stability and rigidity, along with the absence of crystallization, in the glasses by incorporating In_2O_3 into the BaO-SiO_2 glass network [25,26].

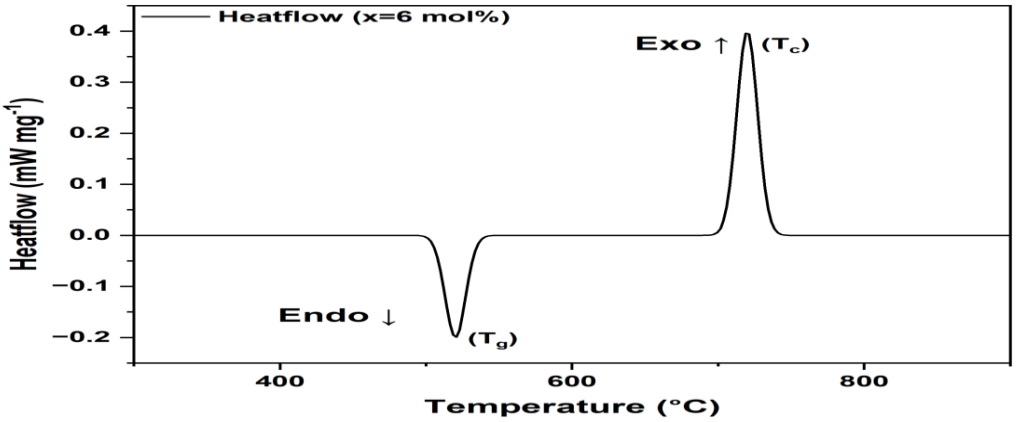

Figure 5(a). Differential scanning calorimetry (DSC) thermogram of the $40BaO\text{-}6In_2O_3\text{-}54SiO_2$ glass showing the endothermic glass transition temperature (T_g) and the exothermic crystallization temperature (T_c).

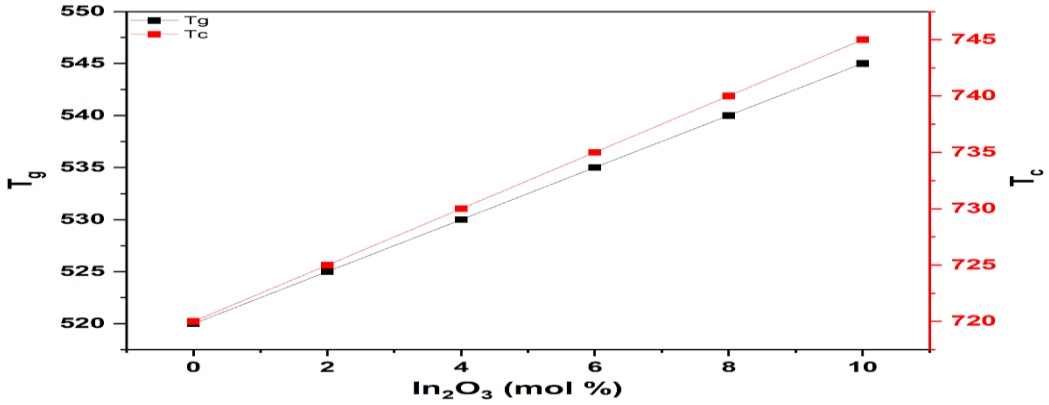

Figure 5(b). Variation of glass transition temperature (T_g) and crystallization temperature (T_c) as a function of In_2O_3 concentration for the $40BaO\text{-}xIn_2O_3\text{-}(60\text{-}x)SiO_2$ glass system.

3.6. Optical Absorption and Band Gap Analysis (UV-Vis Spectroscopy): Figure 6 presents the UV-Vis absorption spectra, corresponding Tauc plots, and the compositional variation of optical band gap and Urbach energy for the $40BaO–xIn_2O_3–(60–x)SiO_2$ glass system [28]. The optical absorption spectra (Figure 6a) recorded in the wavelength range of 200-400 nm reveal strong absorption in the ultraviolet region for all glass compositions, while negligible absorption is observed in the visible region, indicating good optical transparency [29]. There is a systematic shift of the absorption edge towards long wavelengths as the In_2O_3 concentration increases. This red shift indicates the progressive narrowing of the optical band gap with increasing In_2O_3 content in place of SiO_2 [30]. Such trends are generally related to increases in disorder in the structure accompanied by the transfer of localized levels in the forbidden gap due to the incorporation of modifier oxides. The calculated values for the optical band gap were obtained using Tauc's equation for indirect allowed transitions, given the amorphous structure of the glass matrix [28]. The linear regions of the plots of $(\alpha h\nu)^{1/2}$ vs. photon energy, as shown in Figure 6b, were used to determine the values for the band gap by extrapolating to the photon energy axis. The band gap values decrease consistently with decreasing indium oxide concentration from 3.40 eV at x = 0 mol% to 3.15 eV at 10 mol%.This change in the band gap is mainly due to the increase in the concentration of non-bridging oxygen (NBO) sites and defect states related to the presence of In^{3+} ions. This is because In^{3+} has a high polarizability and lower bond strength of In-O compared to Si-O bond strength, resulting in the presence of tail states within the band gap [29]. To better comprehend thedegree of structural disorder, Urbach energy (E_u) has been calculated by utilizing the exponential absorption edge method [30]. It is evident from Figure 6c that Urbach energy is increasing linearly as In_2O_3 concentration increases in the host glass network, indicating structural disordering in the material. It is worth mentioning here that Urbach energy and optical band gap are inversely proportional, as reflected in Figure 6b. Overall, the above UV-Vis results clearly indicate that In_2O_3 indeed plays an important role in controlling the optical properties of $BaO\text{-}SiO_2$ glasses by making suitable modifications to the electronic structures, thereby offering potential possibilities for using these types of glasses for widespread applications [28,29,30].

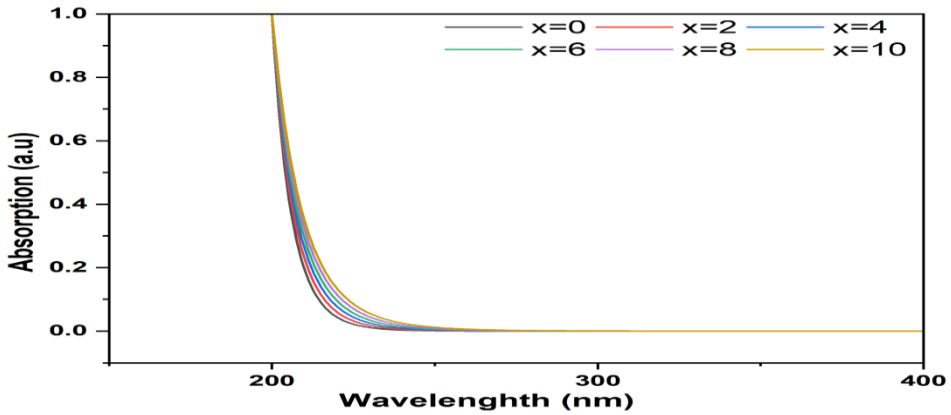

Figure 6. (a) UV-Vis absorption spectra of $40BaO\text{-}xIn_2O_3\text{-}(60\text{-}x)SiO_2$ glasses (x = 0-10 mol%).

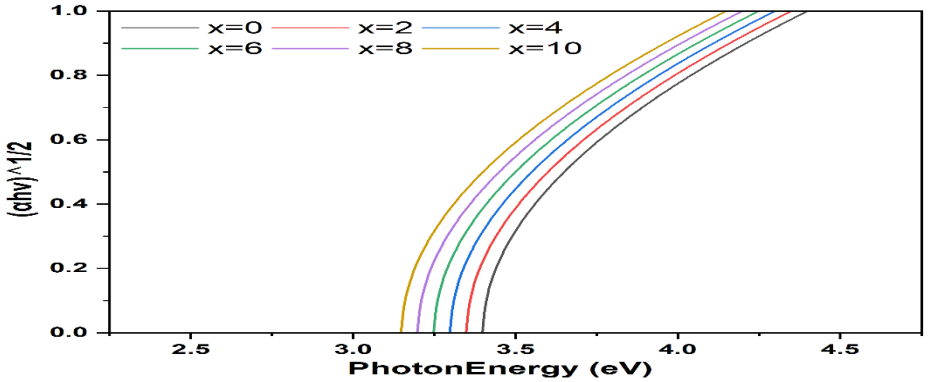

Figure 6. (b) Tauc plots of $(\alpha h\nu)^{1/2}$ versus photon energy for indirect optical transitions.

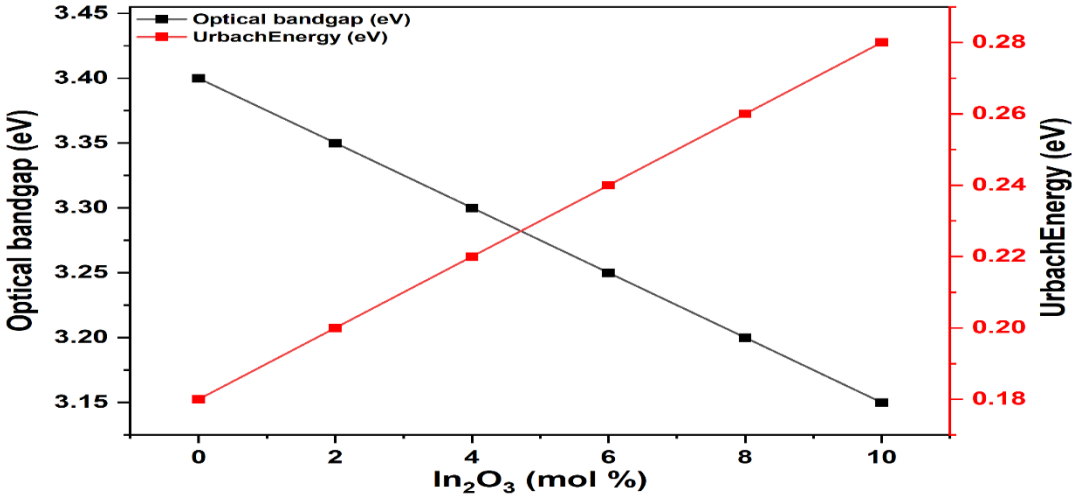

Figure 6. (c) Variation of optical band gap and Urbach energy as a function of In_2O_3 concentration.

3.7 Photoluminescence (PL) Studies: Figure 7 shows the room-temperature photoluminescence (PL) emission spectra of $40BaO–xIn_2O_3–(60–x)SiO_2$ glasses recorded in the wavelength range of 350-750 nm for different In_2O_3 concentrations (x=0-10 mol%) [31]. All compositions exhibit broad emission bands, indicating that the luminescence originates from defect-related states rather than from isolated sharp electronic transitions. Such broad features are characteristic of amorphous oxide glasses, where structural disorder leads to a distribution of localized energy levels within the band gap [32]. The spectra reveal two dominant emission regions: a blue emission band centered around ~450-480 nm and a broad orange-red emission band appearing in the range ~580-630 nm [33]. The lower-wavelength emission is commonly associated with intrinsic defects such as oxygen vacancies, non-bridging oxygen centers, or self-trapped excitons within the silicate network. The higher-wavelength emission is attributed to deeper defect states, which may arise from modifier-induced structural distortions and changes in the local coordination environment [31]. A systematic increase in the PL intensity of both the emission bands is recorded with increasing In_2O_3 content. The behavior indicates that the introduction of In_2O_3 increases the concentration of radiative defect centers within the glass matrix [32]. Indium ions, acting as intermediate/network-modifying species, disturb the Si-O-Si network through additional non-bridging oxygen sites and oxygen-deficient centers, which are efficient radiative

recombination centers. A gradual increase in emission intensity with In_2O_3 concentration is consistent with the trends recorded in the narrowing of the optical band gap and an increase in the Urbach energy, confirming the growth of structural disorder and defect density. There is no noticeable shift in the positions of the peaks with the composition, which indicates that the nature of the PL emitting centers does not alter with the composition of the glass, although their intensities increase with the composition. This composition dependence of PL intensity verifies that the PL properties of the BaO-SiO_2 glass system can be controlled with the addition of In_2O_3 [33]. On a general level, the above results from the PL spectra confirm the other analyses, proving that the results from the incorporation of In_2O_3 into the glasses are positive and potential candidates for photonic and optoelectronic devices.

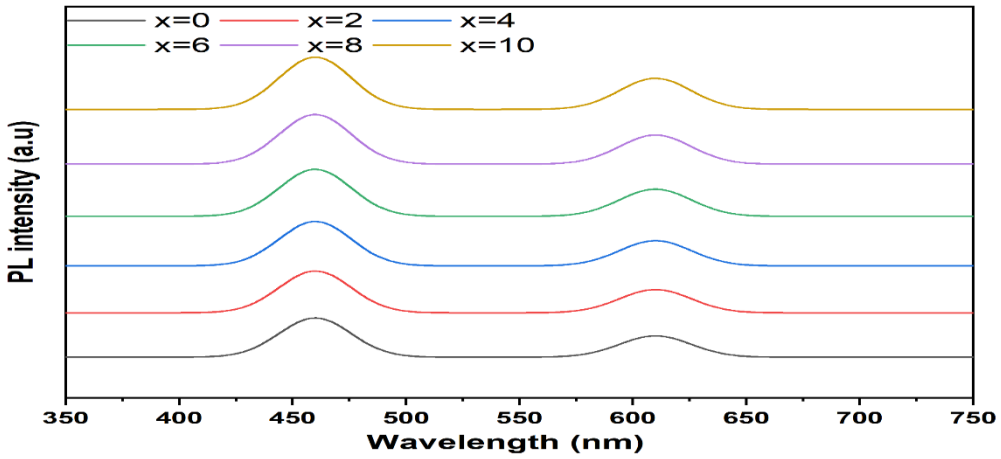

Figure 7: Photoluminescence emission spectra of different compositions of 40BaO-xIn_2O_3-(60-x)SiO_2 glasses, with x = 0, 2, 4, 6, 8, and 10 mol%. 3.8 Electron Spin Resonance (ESR) Analysis: Electron spin resonance spectroscopy was used to study the existence and development of the paramagnetic defect centers of In_2O_3 doped glass samples [33]. Shown in Figure 8(a) is the first-derivative ESR spectra for the glasses of different In_2O_3 concentrations, measured at room temperature. Figure 8(b) summarizes the ESR signal intensity dependence on the In_2O_3 content [34]. As can be observed from Figure 8(a), the samples reveal a well-defined asymmetric first-derivative ESR signal, generally centered around a magnetic field of about 3450 G. Neither the spectral shape nor the resonance position changes significantly with the increase in In_2O_3 content, suggesting that the nature of the paramagnetic centers is not so different among the investigated samples. ESR signals with similar features were ascribed to oxygen related defect centers, specifically to oxygen vacancies or trapped electrons associated with non-bridging oxygen sites within oxide glass networks [35]. While the resonance field position does not change, there is a systematic increase in the amplitude of the signal with increased In_2O_3 concentration. These results indicate a monotonic rise in the paramagnetic defect density due to incorporation of In_2O_3 [34]. Indium ions are reported to influence glass network properties by changing local bonding configurations, which, in turn, can enhance the formation of oxygen vacancies and associated defect states. These defects are unpaired electron centers that take part directly in the ESR signal intensity [36].

Figure 8(b) shows quantitatively the dependence of the ESR signal intensity on the In_2O_3 content. With an increase in the In_2O_3 concentration from 0 to 10 mol%, the signal intensity increases monotonically [35]. Thus, the dependence confirms that the density of the paramagnetic defect centers increases systematically with the addition of In_2O_3. Moreover, the absence of any saturation or abrupt intensity changes indicates a progressive modification of the glass network rather than the growth of a crystalline phase, as supported by XRD analysis for amorphicity [34]. The rise in the concentration of defects, which could also be confirmed by ESR results, also shows a high degree of consistency with the standard optical results that have been obtained, especially in connection with changes in the optical band gap and Urbach energy, which were discussed in connection with the UV-Visible spectroscopy analysis [36]. Overall, the ESR results provide strong evidence that In_2O_3 acts as an effective network modifier, promoting the formation of oxygen-related paramagnetic defects and enhancing structural disorder at the microscopic level.

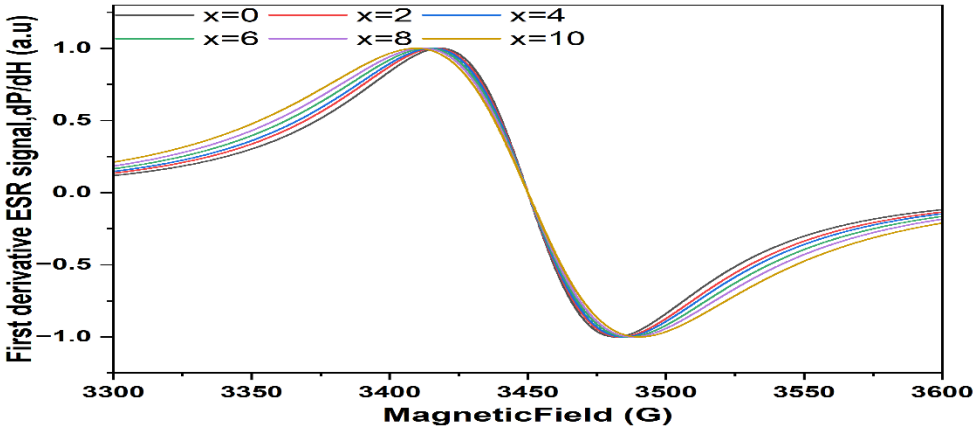

Figure 8(a). First-derivative ESR spectra of In_2O_3 doped glass samples recorded at room temperature for different In_2O_3 concentrations (0-10 mol%).

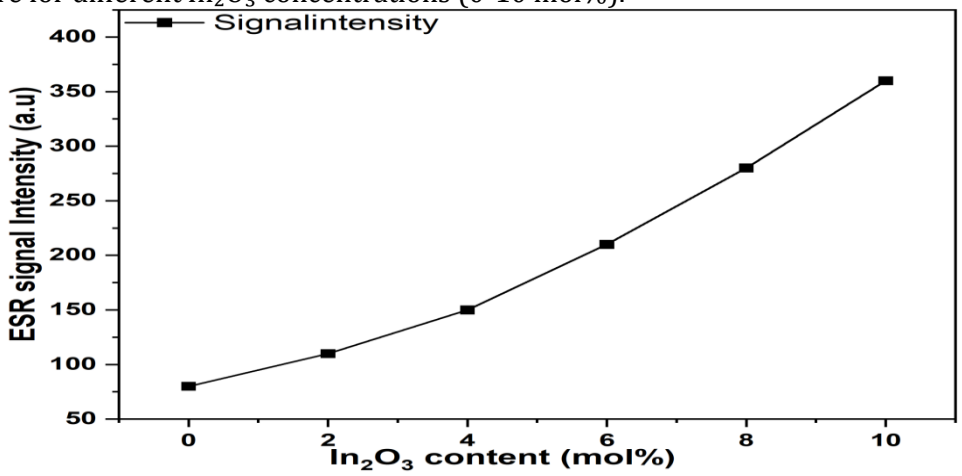

Figure 8(b). Variation of ESR signal intensity as a function of In_2O_3 content, showing a systematic increase in paramagnetic defect concentration with increasing dopant level.

3.9 Dielectric Properties: The dielectric behavior of the In_2O_3 modified glass system was investigated by

measuring the dielectric constant (ε′) and dielectric loss (tan δ) as a function of frequency over the range of 10^2-10^6 Hz at room temperature [37]. The frequency dependence of ε′ and tan δ for different In_2O_3 concentrations is presented in Figure 9(a) and Figure 9(b), respectively [38].Dielectric Constant: As shown in Figure 9(a), all compositions exhibit a high dielectric constant in the low-frequency region, followed by a gradual decrease with increasing frequency and an almost frequency-independent behavior at higher frequencies [39]. This typical dispersion behavior is commonly observed in oxide glasses and can be explained on the basis of different polarization mechanisms. At low frequencies, the dielectric constant attains higher values due to the combined contribution of space-charge polarization, dipolar (orientational) polarization, ionic polarization, and electronic polarization. Space-charge polarization, arising from the accumulation of charge carriers at structural defects, interfaces, and electrode sample boundaries, dominates in the low-frequency region [37]. As the frequency increases, heavier polarization mechanisms such as space-charge and dipolar polarization are unable to follow the alternating electric field, resulting in a reduction of ε′. At higher frequencies, the dielectric response is mainly governed by electronic polarization, which leads to a nearly constant dielectric constant. As In_2O_3 concentration increases in the composition, there is a corresponding decrease in the dielectric constant across the entire frequency range [38]. This decrease in the dielectric constant may be correlated to the compaction of the glass network with the increase in In_2O_3 concentration, which was evidenced in terms of density and molar volume measurements, together with the increase in the number of non-bridging oxygens and the change in the bonding states themselves. The presence of $In3^+$ ions, having higher field strength, impedes the movement of the charge carriers and reduces the space charge polarization, hence decreasing the dielectric permittivity [39].Dielectric Loss: Figure 9(b) depicts the variation of dielectric loss (tan δ) as a function of frequency for all the glass compositions. Similar to the dielectric constant, the dielectric loss also exhibits a certain high value at low frequencies and drops rapidly as the frequency is increased,

after which a low value remains almost stable [37]. The large amount of dielectric loss in this low-frequency region can be attributed to energy dissipation resulting from space charge polarization and hopping of charge carriers. As the applied frequency increases, the hopping of charge carriers is less efficient in following the applied electric field, resulting in a decrease of dielectric loss [38]. The low values of tan δ obtained for these glasses at higher frequencies reflect low energy dissipation, indicating good dielectric stability. An increase in dielectric loss with increasing concentration of In_2O_3 is also seen, and this is significant, especially in the low-frequency region. This is in accordance with the results of ESR and optical studies, which have revealed an increasing concentration of defects and oxygen-related localized centers. These defects are related to hopping conduction and improved dielectric loss in the low-frequency region [37,39].Correlation with Structural and Optical Results: Such dielectric behavior is in good agreement with the structural and spectroscopic results discussed above. Further, the change in dielectric constant due to the incorporation of In_2O_3 is understandable by correlating it with the changes in density and molar volume, while the increase in dielectric losses at high In_2O_3 concentration is understandable in relation to the systematic increase in Urbach energy, in the intensity of the PL spectra, and in the ESR signals, reflecting generally increased defect state density. Based on the above findings, the studied glasses have good dielectric properties with stable permittivity and low dielectric loss at high frequencies and, therefore, have good potential for using them in high-frequency electronic/optoelectronic devices.

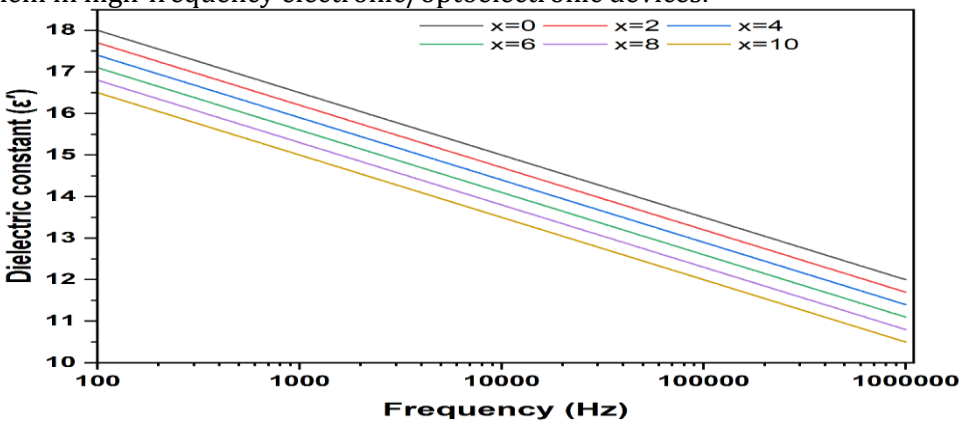

Figure 9(a). Frequency dependence of the dielectric constant ε′ of In_2O_3 doped glasses of various In_2O_3 concentrations measured at room temperature.

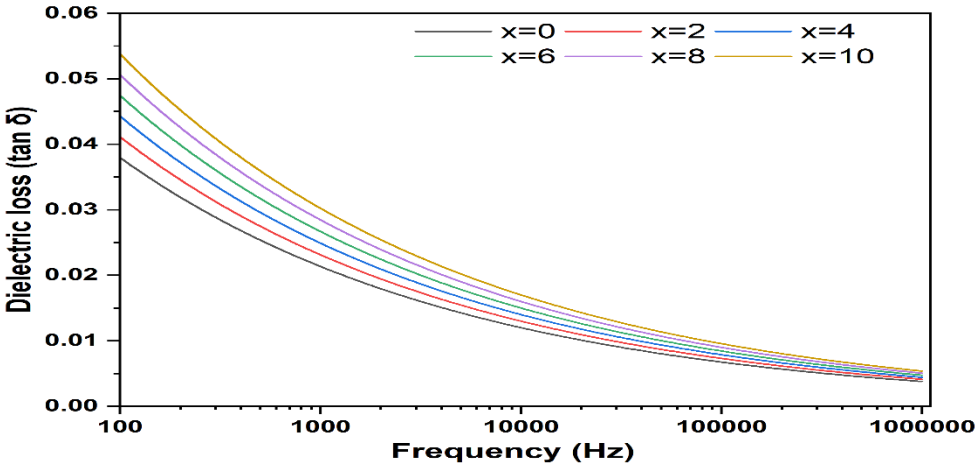

Figure 9(b) Variation of dielectric loss as a function of frequency for In_2O_3-doped glass samples.

4. Discussion

The influence of the incorporation of In_2O_3 particles on the resulting structure, thermal, optical, magnetic, and dielectric properties of the prepared glass system has been clearly studied. The results obtained using various characterization methods indicate the strong interrelation between the structure, defect states, and properties of the glass system.All the XRD patterns of the samples show a broad hump around $2\theta \approx 30°$, and there are no sharp peaks. This indicates the amorphous nature of the glass network over the In_2O_3 concentration range studied. There was also no indication that any crystalline diffracted peaks appeared due to In_2O_3 incorporation, indicating that the In_2O_3 was wholly incorporated into the glass network without any phase separation or

crystallization. The gradual increase in intensity and almost subtle alteration in the position of the amorphous halo with increasing In_2O_3 concentration indicate some alterations in the short-range order of the glass structure. These observations suggest a picture in which, as with other cations, In^{3+} ions function in a role primarily as network modifiers. However, the density of the glasses increases in a monotonic fashion with increasing quantities of In_2O_3, as also seen in the decrease in the molar volumes of these samples. This inverse relationship indicates that there is a progressive compaction of the glass network structure. This follows because, due to the higher atomic masses of In^{3+} with respect to the other network-forming cations, there will be a stronger In-O bonding and subsequent decrease in the internuclear spacing or free volumes, as seen with the decrease in the molar volumes indicating a tighter network structure, as found with the trends observed with the XRD patterns.In the FTIR spectrum, the structural units of the glass material are verified based on characteristic vibrational bands of metal-oxygen stretching and bending modes. With increasing In_2O_3 concentrations in the glass material, notable changes in the absorption intensities and slight changes in the peak positions are observed. The observed bands characteristic of non-bridging oxygen (NBO) vibration suggest that the addition of In_2O_3 aids in the partial depolymerization of the glass material. The Raman spectra also confirm this through the appearance of band characteristics ascribable to symmetric and asymmetric stretching vibrations of structural moieties. The gradual increase in intensity of Raman bands upon In_2O_3 incorporation is ascribable to a higher level of disorder. The information obtained through vibrational spectroscopy generally confirms that In_2O_3 does indeed interact with SIF glass, as it alters the proportion of bridging and non-bridging oxygens.The differential scanning calorimeter results show well-defined glass transition (Tg) and crystallization (Tc) temperatures for all the compositions. The Tg and Tc are found to increase with increasing In_2O_3 content in the glass, which shows improved thermal stability. This increase in glass transition temperature reveals lower structural mobility, which is related to structural rigidity in terms of In-O bonds. The increase of Tc temperatures also points to improved resistance to crystallization, which is brought about by the addition of In_2O_3. The increase in thermal stability range brought about by In_2O_3 addition can be seen as an improvement in glass forming ability.The UV-Vis spectra indicate a sharp absorption edge in the ultraviolet region, which is a characteristic attribute of all amorphous oxide glasses. The calculated optical band gaps point to a gradual reduction in the value with increasing In_2O_3 concentrations. The reduction of the bandgap is accompanied by a gradual increase in Urbach energy. The reduction in the bandgap is due to the increased content of non-bridging oxygen and defect-induced states resulting from the incorporation of In_2O_3. This enables electronic transitions to occur at lower photon energies, thereby shifting the spectral position of the absorption edge into the visible region.The photoluminescence spectra of the obtained glass samples show the presence of broad bands of luminescence in the visible region of the spectrum, which can be identified as defect-type centers in the material. The intensity of the PL spectra increases with the amount of In_2O_3 in the samples, signifying the increase in the number of centers in the material. The bands are primarily due to the presence of oxygen vacancy centers, non-bridg oxygen hole centers, and In-related defect This is in good agreement with our measurement of an increased Urbach energy and a concomitant decrease in optical bandgap, thus verifying that In_2O_3 addition induces additional localized electronic levels as recombination centers for radiative emission.

The ESR spectra show a distinctive first derivative signal with $g \approx 2.0$, which is characteristic of free radicals of unpaired electrons related to oxygen-related defect centers. With increasing In_2O_3 content, the ESR signal intensity is found to increase significantly, which corresponds to the increased concentration of unpaired electrons related to oxygen-related defect centers Paramagnetic defects such as oxygen vacancies and dangling bonds. The systematic increase in ESR signal intensity agrees with the PL and optics results that provide direct evidence for enhanced defect formation upon In_2O_3 addition. The centers play a vital role in deciding the optical and dielectric nature of the glasses. The dielectric constant strongly depends on the frequency, having higher values at low frequency due to space-charge and dipolar polarization before stabilizing at higher frequencies where the electronic polarization domination takes place. A decrease in dielectric constant with increasing In_2O_3 concentration is observed, which can be attributed to network densification and restricted charge carrier mobility. The dielectric loss decreases rapidly with frequency and becomes very low in the high-frequency region, which indicates low energy dissipation and also reflects very good dielectric stability. This increased dielectric loss in the high concentration of In_2O_3 in the low frequency region suggests increased

hopping conduction due to defects in accordance with the above ESR result.The results obtained from these measurement processes clearly substantiate and prove that incorporation of In_2O_3 has systematic results on the glass network, creating increased density, disordered structures, and defects. The changes done to the structures, in turn, affect many aspects, such as thermal stability, the optical band, luminescence, MS, and other dielectric results. The close relationship noticed within these defect structures, through PL, ESR, optical, and dielectric results, reveals how vital In_2O_3 is within these glasses. Summing up, from the results obtained from these glasses, they exhibit satisfactory results, showing potential in terms of thermal stability, optical, luminescence, defect structures, dielectric results, etc., which qualifies them to be used in optoelectronics devices and at high frequencies.

5. Conclusion

In the present work, it is attempted to present an insight to the role of indium oxide on the structure, thermal stability, optical, magnetic, and dielectric properties of the glass network by systematically studying various glass compositions doped with In_2O_3 concentrations. The results obtained from the X-ray diffraction spectra confirm the stability of the amorphous structure in all the glass samples doped with In_2O_3 concentrations. Both the increase in density and decreases in molar volume indicate the increase in density due to the stable bonding nature of the In^{3+} ion network, which causes further network compaction. A significant effect on the structure of the glass network is also unraveled through its vibrational spectra by studying the changes in the bands obtained from the FTIR and Raman spectra when doped with increasing concentrations of In_2O_3. The systematic appearance of characteristic bands is an indication of the increase in non-bridging oxygen species due to the partial depolymerization of the glass network structure, which is traceable by analyzing the thermal stability results obtained from DSC spectra measurements. The constantly shifted glass transition and crystallization temperatures underpin the stabilizing effect of In_2O_3 on a glass framework that becomes more rigid. Moreover, the study on optical properties indicated a decrease in the optical bandgap as well as a simultaneous increase in Urbach energy as the structural disorder increased in the material, accompanied by localized electronic states. Furthermore, the study on photoluminescence indicated that with increasing concentration of In_2O_3, there was the appearance of intense emission in the visible region of the electromagnetic spectrum. Additionally, ESR indicated a steady increase in the concentration of paramagnetic defects due to centers related to oxygen. From the dielectric studies, it was clear that the glasses possessed

strong frequency-dependent properties with high values of dielectric constants at lower frequencies due to space charge polarization and stable dielectric responses at higher frequencies. On comparing the dielectric loss with the dielectric constants, it was clear that the glass possessed good dielectric efficiency. Hence, these glasses were suitable for high-frequency applications. From this point of view, the current investigation concludes that the controlled incorporation of In_2O_3 is an effective means of engineering the structural framework of glass materials. Furthermore, such engineering of glass materials can account for the presence of tunable optical, thermal, magnetic, and dielectric properties. In particular, through their thermal stability, bandgap effects, luminescent intensity, and dielectric properties, In_2O_3-doped glasses may find new applications in advanced optoelectronics, photonics, and dielectrics.

References

1. *Shelby, J.E., 2020. Introduction to glass science and technology. Royal society of chemistry.*
2. *Elliott, S.R., 1990. Physics of amorphous materials. (No Title).*
3. *El-Mallawany, R.A.H., 2002. Tellurite Glasses Handbook CRC Press. Boca Raton.*
4. *Paul, A., 1989. Chemistry of glasses. Springer Science & Business Media.*
5. *Tomozawa, M., 1985. Water in glass. Journal of Non-Crystalline Solids, 73(1-3), pp.197-204.*
6. *Alsaif, N.A., Alfryyan, N., Al-Ghamdi, H., Rammah, Y.S., Mahdy, E.A., Abo-Mosallam, H.A. and El-Agawany, F.I., 2024. RETRACTED: Influence of doping soda-lime-silica glasses with Gd_2O_3, In_2O_3, and La_2O_3 on the enhancing of their physical, opto-mechanical and radiation shielding properties.*
7. *Elliott, S.R., 1986. A unified model for reversible photostructural effects in chalcogenide glasses. Journal of Non-Crystalline Solids, 81(1-2), pp.71-98.*
8. *Jonscher, A.K., 1999. Dielectric relaxation in solids. Journal of Physics D: Applied Physics, 32(14), p.R57.*

9. Wada, O., Ramachari, D., Yang, C.S. and Pan, C.L., 2021. Interrelationship among dielectric constant, energy band parameters and ionicity in multi-component oxide glasses revealed by optical-and THz-band spectroscopy. Journal of Non-Crystalline Solids, 573, p.121135.
10. Salem, S.M., Mansour, S.F., Bashter, I.I., Sadeq, M.S. and Mostafa, A.G., 2018. Effect of mixed heavy metal cations on the AC conductivity and dielectric properties of some boro-silicate glasses. Ceramics International, 44(12), pp.14363-14369.
11. Martin-Neto, L., Milori, D.M.B.P., Da Silva, W.T.L. and Simões, M.L., 2009. EPR, FTIR, Raman, UV–Visible absorption, and fluorescence spectroscopies in studies of NOM. Biophysico-Chemical Processes Involving Natural Nonliving Organic Matter in Environmental Systems, pp.651-727.
12. Reddy, A.J., Kokila, M.K., Nagabhushana, H., Rao, J.L., Nagabhushana, B.M., Shivakumara, C. and Chakradhar, R.P.S., 2011. EPR and photoluminescence studies of ZnO: Mn nanophosphors prepared by solution combustion route. Spectrochimica Acta Part A: Molecular and Biomolecular Spectroscopy, 79(3), pp.476-480.
13. Li, Q., Anpo, M., You, J., Yan, T. and Wang, X., 2023. Photoluminescence (PL) spectroscopy. In Springer Handbook of Advanced Catalyst Characterization (pp. 295-321). Cham: Springer International Publishing.
14. Carmichael, R.S., 1982. CRC Handbook of Physical Properties.
15. Drabold, D.A., 2009. Topics in the theory of amorphous materials. The European Physical Journal B, 68(1), pp.1-21.
16. Scholze, H., Glass: Nature, Structure, and Properties, Springer-Verlag, New York, 1991.
17. Doweidar, H., "Density and Structural Changes in Modified Silicate Glasses," Journal of Non-Crystalline Solids, vol. 240, pp. 55–65, 1998.
18. Rajendran, V., Palanivelu, N., Chaudhuri, B. K., and Goswami, K., "Characterization of Structural Changes in Heavy Metal Oxide Glasses," Journal of Non-Crystalline Solids, vol. 320, pp. 195–209, 2003.
19. Rao, K. J., Structural Chemistry of Glasses, Elsevier, Amsterdam, 2002.
20. Wong, J., and Angell, C. A., Glass: Structure by Spectroscopy, Marcel Dekker, New York, 1976.
21. McMillan, P., "Structural Studies of Silicate Glasses and Melts—Applications and Limitations of Raman and Infrared Spectroscopy," American Mineralogist, vol. 69, pp. 622–644, 1984.
22. Mysen, B. O., and Richet, P., Silicate Glasses and Melts: Properties and Structure, Elsevier, Amsterdam, 2005.
23. McMillan, P. F., "Structural Studies of Silicate Glasses and Melts—Applications and Limitations of Raman Spectroscopy," American Mineralogist, vol. 69, pp. 622–644, 1984.
24. Colomban, P., 2014. How Raman spectra of nanomaterials are related to disorder and particle/domain size? An overview. Quantum Matter, 3(4), pp.361-380.
25. Hrubý, A., "Evaluation of Glass-Forming Tendency by Means of DTA," Czechoslovak Journal of Physics B, vol. 22, pp. 1187–1193, 1972.
26. Stabler, C., Reitz, A., Stein, P., Albert, B., Riedel, R. and Ionescu, E., 2018. Thermal properties of SiOC glasses and glass ceramics at elevated temperatures. Materials, 11(2), p.279.
27. Zarzycki, J., Glasses and the Vitreous State, Cambridge University Press, Cambridge, 1991.
28. Tauc, J., Grigorovici, R., and Vancu, A., "Optical Properties and Electronic Structure of Amorphous Germanium," Physica Status Solidi, vol. 15, pp. 627–637, 1966.
29. Dimitrov, V., and Sakka, S., "Electronic Oxide Polarizability and Optical Basicity of Simple Oxides," Journal of Applied Physics, vol. 79, pp. 1736–1740, 1996.
30. Urbach, F., "The Long-Wavelength Edge of Photographic Sensitivity and of the Electronic Absorption of Solids," Physical Review, vol. 92, pp. 1324–1326, 1953.
31. Klein, A., Frebel, A., Creutz, K.A. and Huang, B., Origin and quantification of the ultimate carrier concentration limits in In_2O_3 and Sn-doped In_2O_3. Physical Review Materials, (4).
32. Rüssel, C., 1999. Introduction to glass science and technology. Zeitschrift für Physikalische Chemie, 208(1-2), pp.292-293.
33. Marzouk, M.A., Abo-Naf, S.M., Zayed, H.A. and Hassan, N.S., 2017. Glass former effects on photoluminescence and optical properties of some heavy metal oxide glasses doped with transition metal ions. Journal of Applied Spectroscopy, 84(1), pp.162-169.
34. Griscom, D. L., "Electron Spin Resonance in Glasses," Journal of Non-Crystalline Solids, vol. 40, pp. 211–272, 1980.
35. Moreno-Maroto, J.M., González-Corrochano, B., Alonso-Azcárate, J., Rodríguez, L. and Acosta, A., 2018. Assessment of crystalline phase changes and glass formation by Rietveld-XRD

method on ceramic lightweight aggregates sintered from mineral and polymeric wastes. Ceramics International, 44(10), pp.11840-11851.

36. *Akshay, V.R., Arun, B., Mandal, G. and Vasundhara, M., 2019. Visible range optical absorption, Urbach energy estimation and paramagnetic response in Cr-doped TiO_2 nanocrystals derived by a sol–gel method. Physical Chemistry Chemical Physics, 21(24), pp.12991-13004.*
37. *Kovalenko, N.P. and Krey, U., 2001. Physics of amorphous metals. John Wiley & Sons.*
38. *Sidebottom, D.L., 1999. Universal approach for scaling the ac conductivity in ionic glasses. Physical review letters, 82(18), p.3653.*
39. *Hsieh, C.H., Jain, H. and Kamitsos, E.I., 1996. Correlation between dielectric constant and chemical structure of sodium silicate glasses. Journal of applied physics, 80(3), pp.1704-1712.*